

Article

Thymoquinone Enhances Paclitaxel Anti-Breast Cancer Activity via Inhibiting Tumor-Associated Stem Cells Despite Apparent Mathematical Antagonism

Hanan A. Bashmail¹, Aliaa A. Alamoudi¹, Abdulwahab Noorwali¹, Gehan A. Hegazy^{1,2}, Ghada M. Ajabnoor¹  and Ahmed M. Al-Abd^{3,4,*} 

¹ Department of Clinical Biochemistry, Faculty of Medicine, King Abdulaziz University, Jeddah 21589, Saudi Arabia; hanan.a.bashmail@gmail.com (H.A.B.); aliaa.alamo@gmail.com (A.A.A.); wal5566@gmail.com (A.N.); gehanhegazy@hotmail.com (G.A.H.); ga_clinbio@yahoo.com (G.M.A.)

² Department of Medical Biochemistry, Medical Division, National Research Centre, Giza 12622, Egypt

³ Department of Pharmaceutical Sciences, College of Pharmacy, Gulf Medical University, Ajman 4184, UAE

⁴ Department of Pharmacology, Medical Division, National Research Centre, Giza 12622, Egypt

* Correspondence: ahmedmalabd@pharma.asu.edu.eg; Tel.: +971-(0)56-464-2929

Academic Editor: Marian Brestic

Received: 4 December 2019; Accepted: 17 January 2020; Published: 20 January 2020



Abstract: Thymoquinone (TQ) has shown substantial evidence for its anticancer effects. Using human breast cancer cells, we evaluated the chemomodulatory effect of TQ on paclitaxel (PTX). TQ showed weak cytotoxic properties against MCF-7 and T47D breast cancer cells with IC₅₀ values of 64.93 ± 14 μM and 165 ± 2 μM, respectively. Combining TQ with PTX showed apparent antagonism, increasing the IC₅₀ values of PTX from 0.2 ± 0.07 μM to 0.7 ± 0.01 μM and from 0.1 ± 0.01 μM to 0.15 ± 0.02 μM in MCF-7 and T47D cells, respectively. Combination index analysis showed antagonism in both cell lines with CI values of 4.6 and 1.6, respectively. However, resistance fractions to PTX within MCF-7 and T47D cells (42.3 ± 1.4% and 41.9 ± 1.1%, respectively) were completely depleted by combination with TQ. TQ minimally affected the cell cycle, with moderate accumulation of cells in the S-phase. However, a significant increase in Pre-G phase cells was observed due to PTX alone and PTX combination with TQ. To dissect this increase in the Pre-G phase, apoptosis, necrosis, and autophagy were assessed by flowcytometry. TQ significantly increased the percent of apoptotic/necrotic cell death in T47D cells after combination with paclitaxel. On the other hand, TQ significantly induced autophagy in MCF-7 cells. Furthermore, TQ was found to significantly decrease breast cancer-associated stem cell clone (CD44+/CD24-cell) in both MCF-7 and T47D cells. This was mirrored by the downregulation of TWIST-1 gene and overexpression of SNAIL-1 and SNAIL-2 genes. TQ therefore possesses potential chemomodulatory effects to PTX when studied in breast cancer cells via enhancing PTX induced cell death including autophagy. In addition, TQ depletes breast cancer-associated stem cells and sensitizes breast cancer cells to PTX killing effects.

Keywords: paclitaxel; thymoquinone; apoptosis; autophagy; tumor-associated stem cells

1. Introduction

Over the past three decades, 1355 new drugs were approved for the treatment of malignancies [1,2]. However, there are 18.1 million new cases of cancer, and 9.6 million mortalities due to cancer annually [3]. Breast cancer has the highest incidence, causing the most female mortalities among other malignancies [4]. Breast cancer tissue is a heterogeneous tissue consisting of various cell types, which differ in terms of origin, function, genetic profile, morphology, and sensitivity to therapy [5,6]. Breast cancer stem cells (BCSCs) are a subclone of cancer cells that have gained great attention,

and are believed to be responsible for tumor growth and unlimited self-renewal ability. BCSCs possess a remarkable ability to effectively persist after exposure to chemotherapy [7].

Paclitaxel (PTX) is anti-microtubule chemotherapy that has been used successfully for different types of solid tumors including breast cancer for more than 40 years [8–10]. PTX stabilizes tubulin dimmers and suppresses microtubule depolymerization during mitosis, resulting in cell cycle arrest in M-phase; it is also called mitotic catastrophe [9,11]. However, breast cancer patients treated with taxane frequently develop chemotherapeutic resistance [12]. Combination therapy for PTX has been studied by many research teams, including ours, to enhance its anti-tumor activity and protect PTX from tumor resistance [13–16].

Natural compounds are believed to be a promising alternative for many chemotherapeutic remedies in fighting neoplasia [17]. More than 74% of the newly approved anticancer drugs during the past 30 years were of natural origin or inspired by natural product [1,2]. *Nigella sativa* and its constituents are among the most studied medicinal herbs in different health care issues [18]. Thymoquinone (TQ) is the major natural component of *Nigella sativa* seeds; it possesses anti-bacterial, anti-oxidant, anti-allergic, and anti-cancer effects [19–22].

Medicinal plants combined with cancer chemotherapy has gained great attention in recent years, and some studies have demonstrated promising results and outcomes. The main goal of these studies was to reduce the chemotherapeutic resistance associated with conventional chemotherapeutic agents or to protect normal tissues from their toxicity [23]. In our previous publications, thymoquinone was shown to improve the activity of cisplatin and gemcitabine against head and neck squamous cell carcinoma and breast cancer cells in addition to protecting oral epithelial cells from cisplatin-induced apoptosis. Herein, we studied the effect of TQ on the cytotoxicity profile of PTX against breast cancer cells, emphasizing breast-cancer-resistant clones in relation to BCSCs.

2. Results

2.1. The Chemomodulatory Effect of Thymoquinone to PTX within Breast Cancer Cells

A sulfarodamine-B (SRB) assay was used to assess the effect of TQ on the cytotoxic profile of PTX against breast cancer cells by calculating the IC_{50} values and R-fractions of single and combined PTX against MCF-7 and T47D cells. PTX showed a dose-dependent cytotoxic effect. Viability started to drop significantly at a concentration of 0.1 μ M with IC_{50} values of $0.2 \pm 0.07 \mu$ M and $0.1 \pm 0.01 \mu$ M in MCF-7 and T47D cells, respectively (Figure 1A,B). In contrary, TQ did not exert any cytotoxic activity against either cell line until 30 μ M. Higher concentrations of TQ induced a sudden drop in the viability with calculated IC_{50} values of $64.9 \pm 14 \mu$ M and $165.1 \pm 2.8 \mu$ M in MCF-7 and T47D cells, respectively (Figure 1A,B). Equitoxic combination (100:1) of TQ with PTX did not further improve the IC_{50} values of PTX against either MCF-7 or T47D cells ($0.7 \pm 0.01 \mu$ M and $0.15 \pm 0.02 \mu$ M, respectively). Combination index analysis showed that TQ antagonized the cell-killing effect of PTX against MCF-7 and T47D cells, resulting in CI-values of 4.6 and 1.6, respectively (Table 1). Yet, TQ completely abolished the resistance fractions of both MCF-7 and T47D towards PTX from $42.37 \pm 1.4\%$ and $41.9 \pm 1.1\%$, respectively, to 0% (Figure 1A,B) (Table 1). These data suggest that TQ does not improve PTX potency against MCF-7 or T47D cells and apparently antagonizes its killing effects. However, TQ significantly abolishes tumor-associated resistant cell clones.

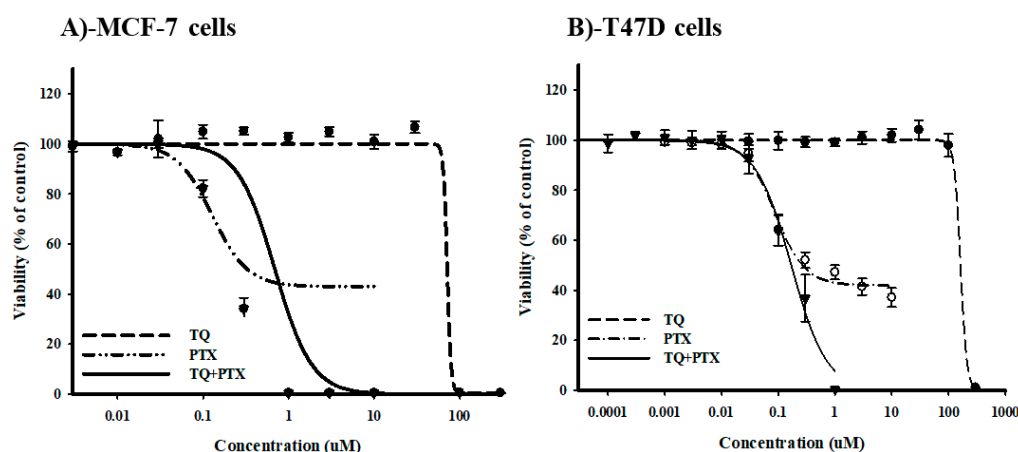


Figure 1. The effect of thymoquinone (TQ) on the dose-response curve of paclitaxel (PTX) in MCF-7 (A) and T47D (B) breast cancer cell lines. Cells were exposed to the serial dilution of PTX, TQ, or their combination for 72 h. Cell viability was determined using a sulfarodamine-B (SRB) assay, and data are expressed as mean \pm SD ($n = 3$).

Table 1. Combination analysis of cell cytotoxicity for TQ, PTX, and their combination against MCF-7 and T47D breast cancer cell lines.

	MCF-7		T47D	
	IC50 (μ M)	R-Value (%)	IC50 (μ M)	R-Value (%)
PTX	0.2 ± 0.07	42.3 ± 1.4	0.1 ± 0.01	41.9 ± 1.1
TQ	64.9 ± 14.5	1.6 ± 1.3	165.1 ± 2.8	0.1 ± 0.15
PTX+TQ	0.7 ± 0.01	0	0.15 ± 0.02	0
CI-value	Antagonism/4.6		Antagonism/1.6	

2.2. Cell Cycle Distribution Analysis of Breast Cancer Cells

Further assessment for the interaction between TQ and PTX against cell cycle progression was undertaken using DNA content flow cytometry. In MCF-7 cells, PTX significantly arrested the cell cycle at G2/M-phase with a significant increase in the G2/M-phase population from $17.5 \pm 2.3\%$ to $71.2 \pm 0.8\%$ and from $15.9 \pm 2\%$ to $72.1 \pm 2.8\%$ after 24 h and 48 h, respectively (Figure 2A,B). TQ alone did not cause any significant change in the cell cycle distribution of MCF-7 cells. However, a combination of TQ with PTX induced a significant increase in the S-phase cell population (from $19.9 \pm 0.5\%$ to $23.8 \pm 1\%$) after 24 h (Figure 2A). The cell cycle arrest at G2/M-phase induced by PTX alone and in combination with TQ resulted in cell death; a significant increase of Pre-G phase population was observed from $4.7 \pm 1.5\%$ to $27.1 \pm 5\%$ and $29.8 \pm 4\%$, respectively, after 24 h (Figure 2C) and from $2.5 \pm 0.6\%$ to $17.9 \pm 1.6\%$, $18.9 \pm 0.4\%$, respectively, after 48 h (Figure 2D).

Similar to MCF-7, PTX significantly arrested T47D cells in G2/M-phase with a significant increase in this population from $19.4 \pm 1.7\%$ to $62.0 \pm 2.9\%$ and from $16.6 \pm 1\%$ to $83.3 \pm 2.1\%$ after 24 h and 48 h, respectively (Figure 3A,B). After 48 h of exposure, TQ alone and TQ+PTX treatment increased the S-phase T47D cell population from $29.1 \pm 1.7\%$ to $38.4 \pm 0.2\%$ and from $15.1 \pm 1.7\%$ to $28.6 \pm 4.1\%$, respectively (Figure 3B). Interestingly, TQ treatment alone induced significant cell death and increased the Pre-G cell population of T47D cells from $8.5 \pm 0.3\%$ to $10.8 \pm 0.2\%$ and from $12.6 \pm 1.4\%$ to $67.6 \pm 5.2\%$ after 24 h and 48 h, respectively (Figure 3C,D). In addition, PTX alone induced a significant increase in the pre-G cell population from $8.5 \pm 0.3\%$ to $38.1 \pm 5.1\%$ and $12.6 \pm 1.45\%$ to $44.5 \pm 3.2\%$ after 24 and 48 h, respectively. Combination of PTX with TQ resulted in a significantly higher pre-G cell population compared to PTX treatment alone after 24 and 48 h ($69.6 \pm 1.1\%$ and $60.4 \pm 1.7\%$, respectively) (Figure 3C,D). Pre-G phase is indicative of cell death. However, it is non-specific and could be programmed cell death (apoptosis or autophagy) or non-programmed cell death (necrosis).

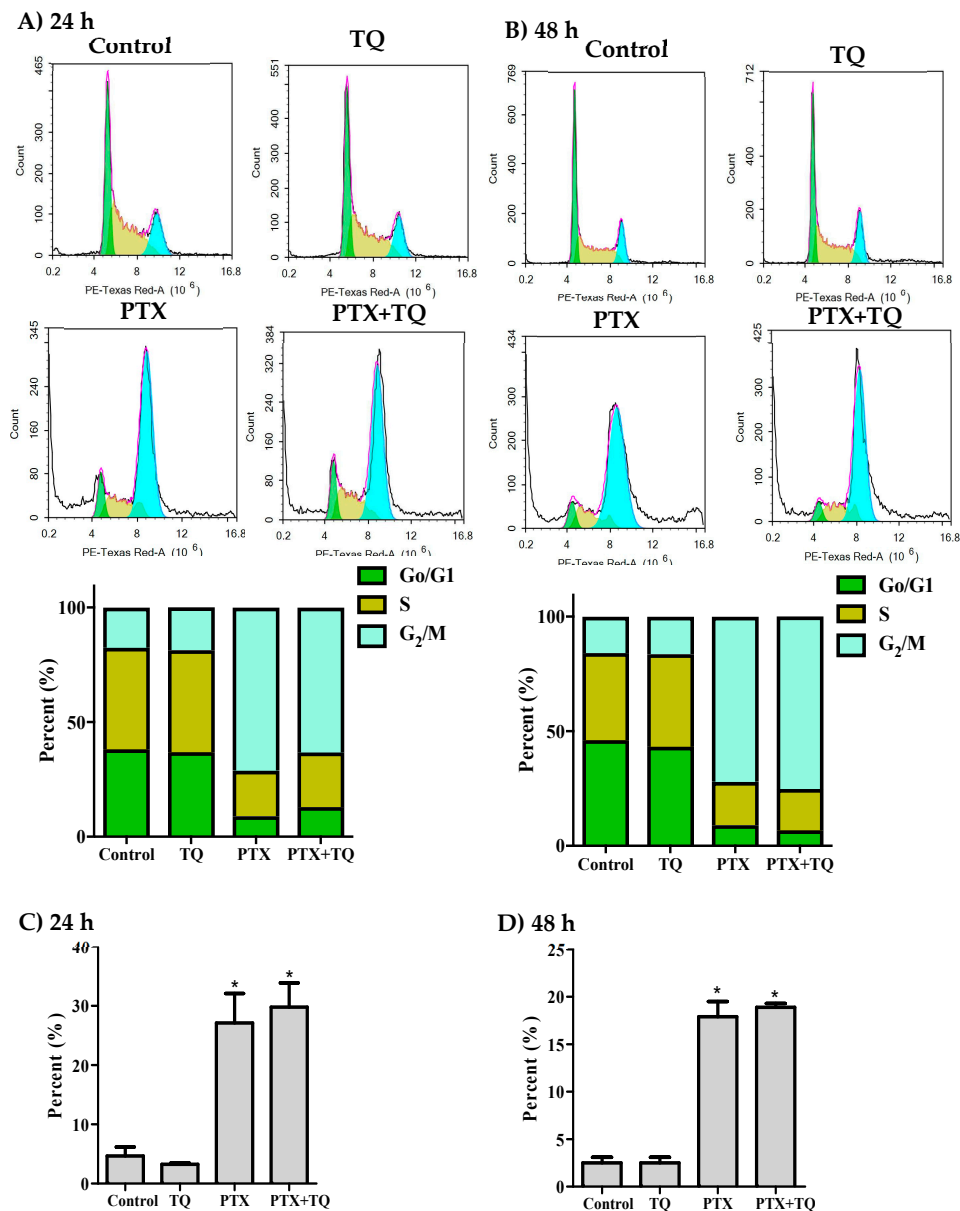


Figure 2. Effect of PTX, TQ, and their combination on the cell cycle distribution of MCF-7 cells. Cells were exposed to PTX, TQ, or their combination for 24 h (A,C) or 48 h (B,D). Cell cycle distribution was determined using DNA content flowcytometry analysis and different cell phases were plotted as percentage of total events. Sub-G cell population was plotted as percent of total events (C,D). Data are presented as mean \pm SD; $n = 3$. (*) significantly different from the control group.

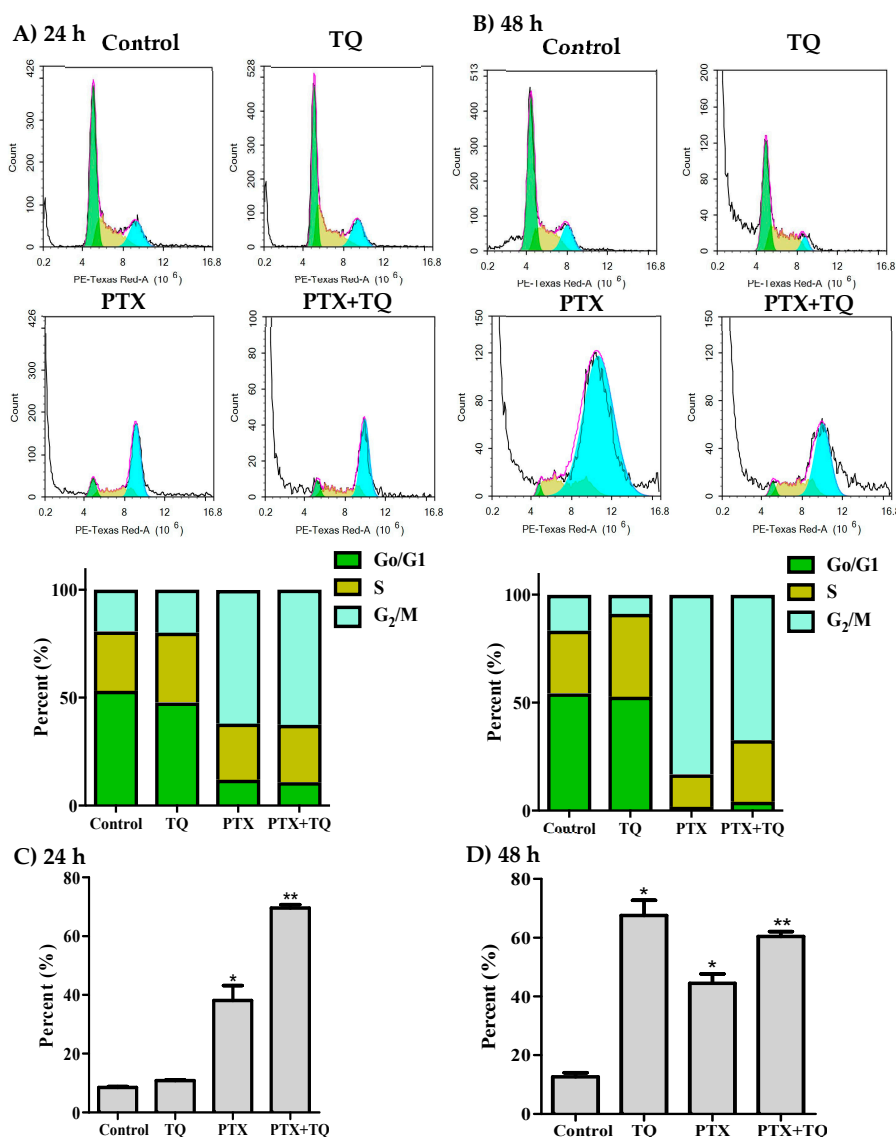


Figure 3. Effect of PTX, TQ, and their combination on the cell cycle distribution of T47D cells. Cells were exposed to PTX, TQ, or their combination for 24 h (A,C) or 48 h (B,D). Cell cycle distribution was determined using DNA content flow cytometry analysis and different cell phases were plotted as percentage of total events. Sub-G cell population was plotted as percent of total events (C,D). Data are presented as mean \pm SD; $n = 3$. (*) significantly different from the control group. (**) significantly different from PTX treatment.

2.3. Apoptosis Assessment

Herein, we investigated the effect of TQ in overcoming MCF-7, T47D cells resistance to PTX by inducing further apoptosis, necrosis, and/or autophagy. T47D cells were exposed to the pre-determined IC_{50} values of PTX, TQ, and their combination for 24 and 48 h rather than 72 h to detect early apoptotic events. Apoptosis/necrosis populations were then determined by Annexin-V/FITC-PI staining coupled with a flow cytometry technique. Both TQ alone and PTX alone induced a significant apoptosis after 24 h of exposure ($22.4 \pm 3.2\%$ and $10.3 \pm 0.8\%$, respectively) compared to untreated control T47D cells ($4.3 \pm 0.5\%$). Yet, PTX combination with TQ induced significantly more apoptosis compared to PTX treatment alone ($58.1 \pm 2.1\%$). In addition to apoptosis, TQ, PTX, and their combination induced significant necrotic cell death in T47D by $5.9 \pm 0.3\%$, $7.4 \pm 0.7\%$, and $22.2 \pm 0.6\%$, respectively (compared to $2.3 \pm 0.7\%$ necrosis in control cells) (Figure 4A)). Similarly, further exposure (48 h) of T47D cells to PTX alone or TQ alone resulted in more apoptosis ($18.4 \pm 2.9\%$ and $32.5 \pm 2.8\%$, respectively) compared

to untreated control cells ($1.9 \pm 0.5\%$). Combination of PTX and TQ did not significantly increase T47D apoptotic cell population compared to TQ treatment alone ($31.5 \pm 1.3\%$). Moreover, TQ, PTX, and their combination induced significant necrotic cell death in T47D by $4.0 \pm 0.4\%$, $11.3 \pm 0.6\%$, and $11.0 \pm 0.4\%$, respectively (compared to $2.6 \pm 0.1\%$ necrosis in control cells) (Figure 4B). To confirm apoptosis, Western blot analysis was carried out for caspase-3 and PARP proteins. PTX induced the expression of caspase-3 after 24 and 48 h. Further combination of PTX with TQ resulted in more active caspase-3 and more cleavage for its downstream target protein, PARP (Figure 4C,D).

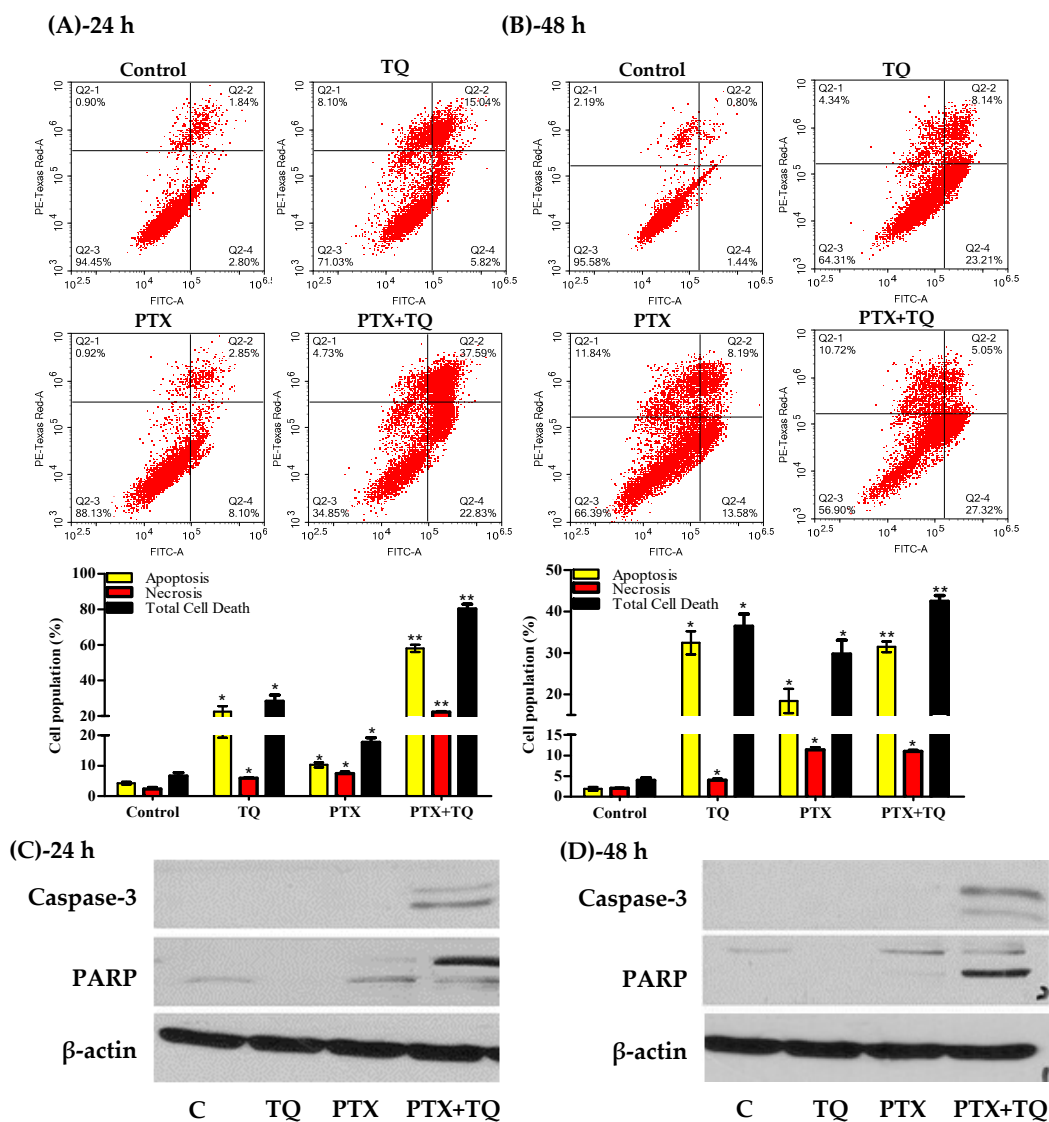


Figure 4. Apoptosis/necrosis assessment in T47D cells after exposure to PTX, TQ, and their combination. Cells were exposed to PTX, TQ, or their combination for 24 h (A) and 48 h (B). Cells were stained with annexin V-FITC/PI and different cell populations are plotted as a percentage of total events. Western blot analysis for caspase-3 and PARP was assessed for MCF-7 (C) and T47D (D) cells. Data are presented as mean \pm SD; $n = 3$. (*) significantly different from the control group. (**) significantly different from PTX treatment.

2.4. Autophagy Assessment

Besides apoptosis, we were keen to study the effect of PTX, TQ, and their combination on other cell death mechanisms such as the autophagy process. In MCF-7, treatment with PTX, TQ, and the combination of PTX+TQ increased the fluorescent intensity indicative of autophagic cell death by 58.2%, 33.9%, and 49.1%, respectively (Figure 5A). On the other hand, none of the treatments under

investigation (PTX, TQ, or their combination) induced any significant change or autophagic cell death in T47D (Figure 5B). CQ (positive control autophagic drug) induced autophagic cell response in MCF-7 and T47D cell lines and increased Cyto-ID fluorescence by 31 and 42%, respectively (Figure 5A,B). For further conformation, two key autophagy genes beclin-1 and LC3-II were assessed by the RT-PCR technique. In MCF-7 cells, treatment with PTX, TQ, and the a combination of PTX+TQ significantly increased the expression of beclin-1 by 4.4, 3.1, and 6.8 folds, respectively, and significantly increased the expression of LC3-II by 3.4, 1.9, and 4.1 folds, respectively. In T47D, only PTX marginally increased the expression of beclin-1 by 1.4 folds (Figure 5C,D)

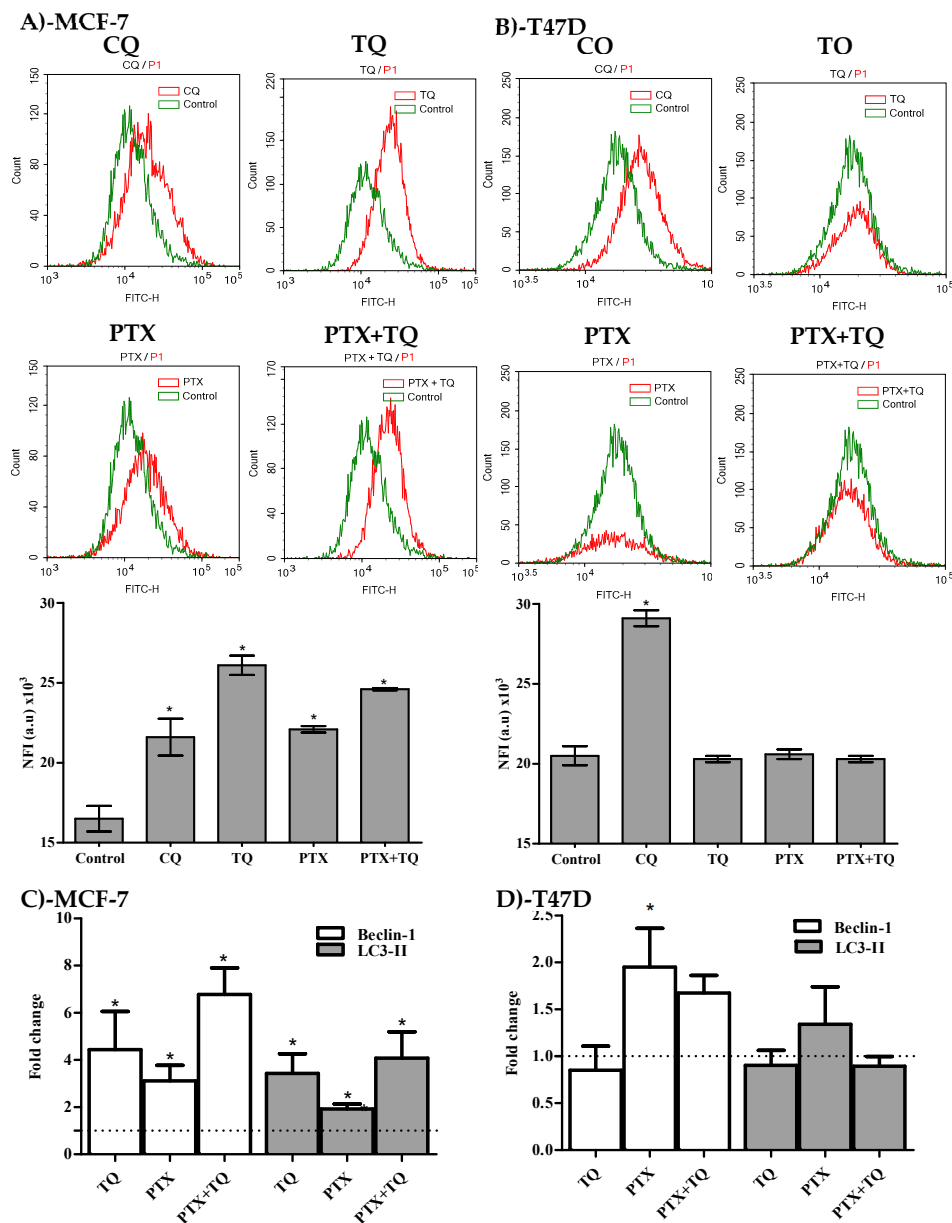


Figure 5. Autophagic cell death assessment in MCF-7 (A) and T47D (B) cells after exposure to PTX, TQ, and their combination. Cells were exposed to PTX, TQ, or their combination for 24 h, and were stained with a Cyto-ID autophagosome tracker. Net fluorescent intensity (NFI) was plotted and compared to the basal fluorescence of the control group. Gene expression fold changes for beclin-I and LC3-II were assessed for MCF-7 (C) and T47D cells (D). Data are presented as mean \pm SD; $n = 3$. (*) significantly different from the control group.

2.5. Breast Cancer-Associated Stem Cell (CD44⁺/CD24⁻ Cell Clone) Detection

Furthermore, we assessed the breast cancer-associated stem cell clone (CD44⁺/CD24⁻) and endothelial mesenchymal transition gene expression in relation to treatment with TQ, PTX, and their combination. TQ alone induced a significant decrease in the CD44⁺/CD24⁻ stem cell clone by $12.4 \pm 0.8\%$. However, PTX treatment reduced CD44⁺/CD24⁻ cell clone by only $7.6 \pm 0.1\%$. Interestingly, the combination of PTX with TQ significantly abolished the tumor-associated stem cell clone (CD44⁺/CD24⁻) by $32.3 \pm 0.08\%$ (Figure 6A). In addition, TQ significantly decreased the T47D associated stem cell clone (CD44⁺/CD24⁻) by $19.9 \pm 0.8\%$, while PTX caused a $9.9 \pm 0.2\%$ decrease in the tumor-associated stem cell clone. Yet, the combination of PTX with TQ further decreased the tumor-associated stem cell clone by $23.9 \pm 1.6\%$ (Figure 6B).

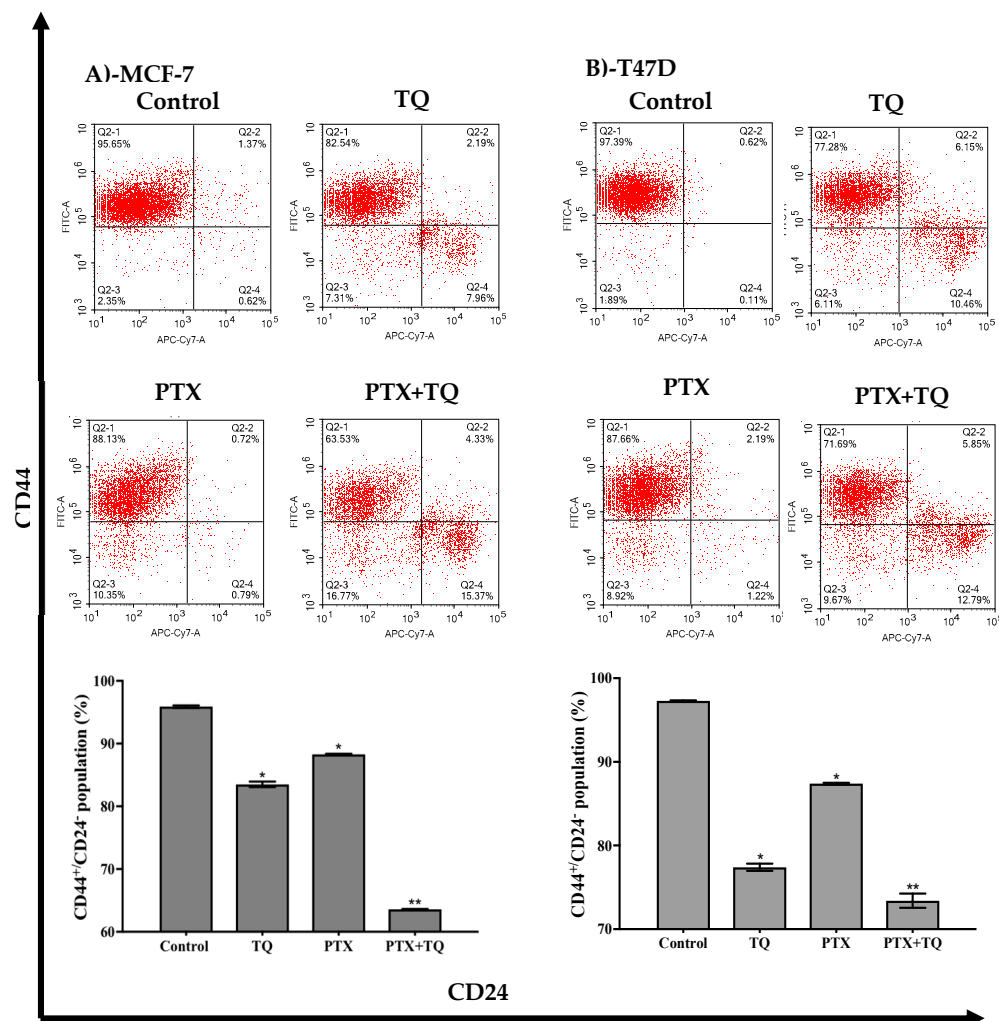


Figure 6. Effect of PTX, TQ, and their combination on the expression of CD44 and CD24 stem cell markers. MCF-7 (A) and T47D (B) cells were exposed to PTX, TQ, or their combination for 24 h. Expression levels of CD44 and CD24 were assessed using flow cytometry and plotted as percentage of total events. Data are presented as mean \pm SD; $n = 3$. (*) significantly different from the control group. (**) significantly different from PTX treatment.

2.6. EMT Genes Expression Assessment

Further assessment for the expression of key EMT genes (ZEB-2, TWIST-1, SNAIL-1, and SNAIL-2) after treatment with TQ and PTX was undertaken using the RT-PCR technique. No significant changes in the expression of ZEB-2 due to the treatment of TQ or PTX could be detected. TQ induced a significant

increase in the expression level of both SNAIL-1 and SNAIL-2 compared to the untreated control by 3.8 and 3.7 folds, respectively. On the other hand, TQ significantly downregulates TWIST-1 expression to 18% of the control expression level. PTX did not induce any significant change in the expression level of the SNAIL-1, SNAIL-2, or TWIST-1 genes. Taken together, TQ efficiently diminishes tumor-associated stem cells (Figure 7).

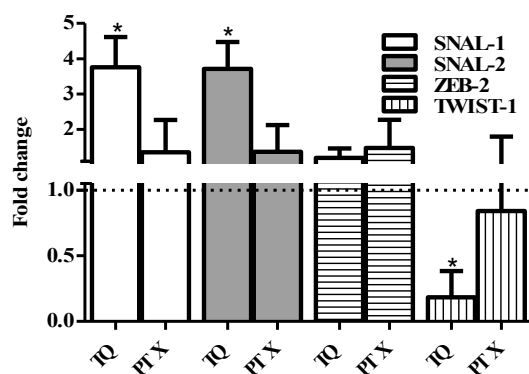


Figure 7. Effect of PTX and TQ on the expression of EMT-related genes in MCF-7 cells. Cells were exposed PTX or TQ for 24 h. Total RNA was extracted and subjected to RT-qPCR to measure gene expression. Data were plotted using the $2^{-\Delta\Delta Ct}$ method (expression normalized to the housekeeping gene GAPDH). Fold expression and significance was calculated relative to control untreated cells (dotted line). Data are presented as mean \pm SD; $n = 3$. (*) significantly different from the control group.

3. Discussion and Conclusion

Breast cancer remains the most common malignancy in females and a leading cause of death worldwide [3,24]. PTX is a cornerstone and commonly used chemotherapeutic drug for the treatment of breast cancer [9,25]. Despite its promising initial clinical response, it might be discontinued due to the emergence of resistance and toxicities [26,27]. TQ is a major active component of the *Nigella sativa* plant, which is commonly used for different medicinal purposes [18,28]. Herein, we are testing the hypothesis that a combination of PTX with TQ can decrease the breast cancer cell resistance to PTX.

According to our data, TQ alone showed significantly weaker cytotoxic/antiproliferative effects compared to PTX. Apparently, TQ combined with PTX resulted in decreased PTX potency in the form of a slight increase in its IC_{50} values. It was interesting to discover that TQ significantly abolished the resistance fractions of both breast cancer cell lines to PTX (R-fractions were above 40% in both cell lines). In one of our previous publications, it was found that curcuminoid-based synthetic compounds increased the IC_{50} of PTX against colorectal cancer cells but significantly decreased the resistance fractions of these cells towards PTX [16]. Herein, we have a similar scenario with the natural and safe compound, TQ. Cumulative evidence within the literature reports the safety and potency of TQ in enhancing many chemotherapeutic compounds against different tumor cell lines [29–32].

It is well known that PTX causes cell cycle arrest in the G2/M phase [33]. According to our finding in the current study, TQ induced accumulation of cells in S-phase. This could explain the apparent antagonism between PTX and TQ. However, this combination resulted in an increase in the pre-G cell population. Yet, TQ pushed quiescent stem cells to proliferate and become sensitized to PTX treatment via entering S-phase temporally and then entering G2/M-phase [34].

The elevated Pre-G cell population due to PTX treatment alone or in combination with TQ is indicative of cell death. Apoptotic, necrotic, and autophagic cell death induced by PTX, TQ, and their combination were examined to test the above hypothesis. Our observations showed that TQ significantly increased apoptosis in T47D cells by more than 4 folds and 16 fold after 24 h and 48 h, respectively. Many previous publications from our team and from others have highlighted the apoptotic effects of TQ against several cancer cells [31,32,35,36]. The enhancement effect of TQ towards PTX against T47D could be explained by the supra increase of apoptosis; PTX in combination with

TQ increased the apoptosis by more than 4 folds compared to PTX alone. It is worth mentioning that combination treatment induced marked elevation rates of necrosis compared to PTX alone. It was previously reported by Canatan and colleagues that the combination of PTX with TQ increased the expression of several genes involved in apoptosis in triple-negative breast cancer [37]. On the other hand, MCF-7 does not undergo normal apoptosis due to a lack of caspase-3 expression [38]. In the current work, caspase-3 was not detected by Western blotting in MCF-7 cells. Yet, it was suggested in our previous publications that autophagy represents an alternative cell death pathway in MCF-7 cells [32]. Herein, TQ induced autophagic pro-death effects in MCF-7 cells. In other words, PTX and TQ increased the concentration of caspase-3 enzyme in T47D cells with a prominent elevation of cleaved PARP concentration, which is indicative of apoptosis-dependent cell death. In MCF-7 (caspase-3 deficient cell line), TQ and PTX forced the cells to proceed in autophagy-dependent cell death.

Breast cancer stem cells play an important role in resisting chemotherapeutic treatments, and targeting or depleting this clone could effectively sensitize cancer cells to drugs [39]. Overall, our results provide further evidence to the ant-resistance effect exhibited by TQ in combination with PTX through studying their effect against breast cancer-associated stem cells (CD44+/CD24-) [40]. To the best of our knowledge, this is the first study demonstrating the effect of TQ in depleting BCSCs. Herein, TQ remarkably decreased the percentage of the CD44+/CD24- cell clone of MCF-7 and T47D, while PTX caused a slight decrease in the CD44+/CD24- cell clone. Interestingly, TQ in combination with PTX significantly decreased the aforementioned clone far more than TQ or PTX treatment alone. Resistance to chemotherapy and poor cancer patient prognosis was previously attributed to the failure of chemotherapy in depleting this stem cell clone [41]. Finally, the TQ effect in depleting tumor-associated stem cells was confirmed via studying the expression levels of key EMT genes. BCSCs possess high expression levels of mesenchymal markers such as TWIST-1 and a low expression of epithelial markers [42]. Herein, TQ significantly downregulates EMT-regulatory protein (TWIST-1) expression. Previously, it was found that TQ downregulates TWIST-1 expression in other tumor types, resulting in improved efficacy [43]. Other key EMT genes, the SNAIL gene family, are known to promote the migration and invasion of cancer cells [44]. Further details showed that the SNAIL family increased the sensitivity to anti-tubulin drugs such as PTX through the downregulation of bIII and bIVa-tubulin [45]. Thus, the observed increased expression of SNAIL1 and SNAIL2 due to TQ treatment, in the current study, provides PTX with a wider target to induce mitotic catastrophe, resulting in ultimately reduced resistance.

In conclusion, TQ proved and is still proving to have a potential effect in chemosensitizing several tumor types such as breast cancer to many chemotherapeutic agents such as PTX. Several aspects of TQ in decreasing breast cancer cell resistance to PTX are shown in this study. Mechanisms underlying this effect include cell cycle synchronization followed by cell death via apoptosis, necrosis, and autophagy. In addition, TQ interacts with EMT properties resulting in diminishing tumor-associated resistant stem cell fraction. Further *in vivo* studies that translate these molecular observations into therapeutic values is highly recommended.

4. Materials and Methods

4.1. Drugs and Chemicals

Thymoquinone (TQ), paclitaxel (PTX), and sulfarodamine-B (SRB) were all obtained from Sigma-Aldrich Chemical Co. Cell culture media, fetal bovine serum, and trypsin were obtained from Gibco™, Thermo Fisher Scientific.

4.2. Cell Culture

MCF-7 and T47D, were obtained from Nawah Scientific (Mokkatam, Cairo, Egypt). Cells were maintained in full DMEM media with heat-inactivated fetal bovine serum (10% *v/v*), streptomycin

(100 µg/mL), and penicillin (100 units/mL). Cells were kept in a humidified, 5% (v/v) CO₂ atmosphere at 37 °C.

4.3. Cell Viability Assay

An SRB assay was used to evaluate the cytotoxicity effect of TQ, PTX, and/or their combination against MCF7 and T47D as previously described. Cells were seeded at 3000–5000 cells/well and treated with a serial concentration of TQ (0.01–300 µM), PTX (0.001–10 µM), and their combination for 72 h. Following that, cells were fixed by adding TCA (10% w/v) to each well and incubated for 1 h at 4 °C. After washing, a 0.4% SRB staining solution (w/v) was added, and the following steps and incubations followed what was previously described. The absorbance was measured at 540 nm with an ELISA microplate reader and calculated as the percent viability of control cells (cells exposed to drug-free media). DMSO concentrations were less than 0.1% in all treatment conditions.

4.4. Data Analysis

The dose–response curves of TQ, PTX, and their combination were analyzed using the E_{max} model [46] according to the following formula

$$\% \text{ Cell viability} = (100 - R) \times \left(1 - \frac{[D]^m}{K_d^m + [D]^m} \right) + R \quad (1)$$

The CI-value was calculated from the following formula:

Combination index (CI) was calculated from the formula:

$$CI = \frac{\text{IC}_{50} \text{ of drug(x) combination}}{\text{IC}_{50} \text{ of drug(x) alone}} + \frac{\text{IC}_{50} \text{ of drug(y) combination}}{\text{IC}_{50} \text{ of drug(y) alone}} \quad (2)$$

The nature of the drug interaction was defined according to Chou and Talalay as synergism if CI < 0.8, as antagonism if CI > 1.2, and as additive if CI ranges from 0.8 to 1.2 [47].

4.5. Cell Cycle Analysis by Flow Cytometry

To evaluate the effect of the drugs on cell cycle distribution, both cell lines were treated by the pre-determined IC₅₀ values of TQ, PTX, or both drugs in combination, for 24 or 48 h. An additional drug-free medium-treated group acted as a control group. Post-treatment, cells were trypsinized, collected, and washed with ice-cold PBS and re-suspended in 0.5 mL of PBS. To ensure fixation of cells, 2 mL of 60% ice-cold ethanol were added on the cells while vortexing. Cells were incubated at 4 °C for 1 h. Prior to analysis, cells were washed and re-suspended in 1 mL of PBS containing 50 µg/mL RNAase A and 10 µg/mL propidium iodide (PI). Cells were incubated for 20 min in the dark at 37 °C and analyzed for DNA content using flow cytometry analysis FL2 (λ_{ex/em} 535/617 nm). In all of the following flow cytometer analysis, 12,000 events were acquired, and NovoExpress™ software was used for analysis.

4.6. Analysis of Cell Apoptosis by Flow Cytometry

An Annexin V-FITC apoptosis detection kit (Abcam Inc., Cambridge Science Park, Cambridge, UK) was used to determine the effect of drugs on apoptosis and necrosis. Briefly, the cells were treated by the pre-determined IC₅₀ values of either TQ, PTX, or both drugs combined for 24 h. A drug-free media-treated group was used as control. Cells were collected and washed twice with PBS and incubated in a dark place with 0.5 mL of Annexin V-FITC/PI solution for 30 min at room temperature according to the manufacturer's protocol. FITC and PI fluorescent signals were then analyzed using FL1 and FL2 signal detector, respectively (λ_{ex/em} 488/530 nm for FITC and λ_{ex/em} 535/617 nm for PI). Positive FITC and/or PI cells were quantified by quadrant analysis.

4.7. Analysis of Cell Autophagy by Flow Cytometry

To further confirm the cell death mechanism induced by the drugs, autophagic cell death was quantitatively analyzed using a Cyto-ID Autophagy Detection Kit (Abcam Inc., Cambridge Science Park, Cambridge, UK). In brief, cells were treated for 24 h by the IC₅₀ values of the test compounds (single or combined treatments). Chloroquine treatment (10 μM) was used as a positive control, while a drug-free medium was used as a negative control. Cells were then washed twice with PBS and stained with Cyto-ID Green in the dark at 37 °C for 30 min according to the manufacturer's protocol. After staining, cells were analyzed for Cyto-ID differential green/orange fluorescent signals using an FL2 signal detector (λ_{ex}/em 535/617 nm). Mean net fluorescent intensities (NFI) were quantified.

4.8. Stem Cell Detection by Flow Cytometry

For assessing the effects of TQ, PTX, and their combination against the breast cancer-associated stem cell clone (CD44+/CD24-), cells underwent FITC-labeled anti-CD44 and APC/Cy7-labeled anti-CD24 antibody (Abcam Inc. Cambridge Science Park, Cambridge, UK) staining and flowcytometry assessment. Briefly, cells were treated with the predetermined IC₅₀ values of test drugs (single or combined treatments), or with drug-free media as a control group, for 24 h. After treatment, cells were trypsinized and washed with ice-cold PBS supplemented with 10% FCS. Cells were stained with the conjugated anti-CD44 and anti-CD24 antibodies and kept in the dark at room temperature for 30 min. Cells were then washed three times with ice-cold PBS containing 10% FCS. Cells were then analyzed for FITC and APC/CY7 fluorescent signals using FL1 and FL2 signal detector, respectively (λ_{ex}/em 488/530 nm for FITC and λ_{ex}/em 535/617 nm for APC/CY7).

4.9. EMT Gene Expression Analysis

Real-time polymerase chain reaction (PCR) was performed to assess the expression of CDH1, CDH2, SNAL1, SNAL2, ZEB2, and TWIST1 genes after treatment with the pre-determined IC₅₀ values of TQ and PTX. After 24 h of treatment, RNA was extracted using mirVana™ RNA isolation kit (Invitrogen, Carlsbad, CA, USA). The RNA and purity were confirmed (A260/280 > 2.0) using a DeNovix DS-11™ microvolume spectrophotometer (Thermo Fisher Scientific, Wilmington, DE, USA). Subsequently, the total RNA samples of all treatments were reverse-transcribed to construct a cDNA library using the SuperScript™ Master Mix kit (Invitrogen, Carlsbad, CA, USA). The cDNA were then subjected to quantitative real-time PCR reactions using Custom TaqMan® Gene Expression Assay (Applied Biosystems, Foster City, CA, USA). GAPDH was used as a housekeeping gene; normalized fold changes for all genes of interest were calculated using the following formula: 2^{-ΔΔC_q}.

4.10. Autophagy Gene Expression Analysis

Real-time polymerase chain reaction (PCR) was performed on the cDNA prepared in the previous experiment to assess the expression of beclin-1 and LC3-II autophagy genes after treatment with the pre-determined IC₅₀ values of TQ and PTX. The beclin-1 forward primer was 3'-GGCTGAGAGACTGGATCAGG-5'; the backward primer was 5'-CTGCGTCTGGGCATAACG-3'; the LC3-II forward primer was 3'-GAGAAGCAGCTTCCTGTTCTGG-5'; the backward primer was 5'-GTGT CCGTTCACCAACAGGAAG-3'. The housekeeping β-actin gene was as a reference gene with a forward primer of 3'-GAGAGCGGCTAAGGTGTTT-5' and a backward primer of 5'-TGGTGTAGACGGGGATGACA-3'.

4.11. Western Blot Analysis and Detection of Apoptosis Related Signals

Apoptosis proteins, caspase-3, and PARP were assessed within cell lysate after treatment with TQ, PTX, and their combination to confirm cell death propagation via apoptosis. Briefly, cells were treated with the pre-determined IC₅₀ values of PTX and TQ for 24 h and 48 h. Cell lysates were extracted using an RIPA-buffer and electrophoresed using SDS-PAGE (10%) and then transferred to PVDF-membrane.

Caspase-3 and cleaved PARP-1 proteins were detected using rabbit monoclonal anti-active caspase-3 and rabbit monoclonal anti-PARP (Abcam Inc., Cambridge Science Park, Cambridge, UK). Bands were visualized using HRP-conjugated anti-rabbit secondary antibodies (Abcam Inc., Cambridge Science Park, Cambridge, UK).

4.12. Statistical Analysis

Data are presented as mean \pm SD using Prism[®] for Windows, ver. 5.00 (GraphPad Software Inc., La Jolla, CA, USA). To assess significance, analysis of variance (ANOVA) with an LSD post hoc test was used with SPSS[®] for Windows, version 17.0.0. A cut off value of $p < 0.05$ was used for significance.

Author Contributions: Conceptualization, A.M.A. Data curation, H.A.B.; Formal analysis, H.A.B., A.A.A., and A.M.A.; Funding acquisition, A.M.A.; Methodology, A.M.A.; Project administration, A.M.A.; Resources, A.A.A. and A.N.; Supervision, A.A.A., A.N., G.A.H., and G.M.A.A.; Validation, G.A.H.; Writing – original draft, H.A.B.; Writing – review & editing, G.A.H., G.M.A.A., and A.M.A.

Funding: This work was supported by the Deanship of Scientific Research (DSR), King Abdulaziz University, Jeddah, Saudi Arabia [grant numbers 303/166/1436].

Conflicts of Interest: The authors declare that there is no conflict of interest. The funders had no role in the design of the study; in the collection, analyses, or interpretation of data; in the writing of the manuscript; or in the decision to publish the results.

Abbreviations

The following abbreviations are used in this manuscript:

BCSC	Breast cancer stem cell
CQ	Chloroquine
PTX	Paclitaxel
SRB	Sulfarodamine-B
TQ	Thymoquinone

References

1. Clardy, J.; Walsh, C. Lessons from natural molecules. *Nature* **2004**, *432*, 829. [[CrossRef](#)] [[PubMed](#)]
2. Newman, D.J.; Cragg, G.M. Natural products as sources of new drugs over the 30 years from 1981 to 2010. *J. Nat. Prod.* **2012**, *75*, 311–335. [[CrossRef](#)] [[PubMed](#)]
3. Bray, F.; Ferlay, J.; Soerjomataram, I.; Siegel, R.L.; Torre, L.A.; Jemal, A. Global cancer statistics 2018. GLOBOCAN estimates of incidence and mortality worldwide for 36 cancers in 185 countries. *CA Cancer J. Clin.* **2018**, *68*, 394–424. [[CrossRef](#)] [[PubMed](#)]
4. Torre, L.A.; Islami, F.; Siegel, R.L.; Ward, E.M.; Jemal, A. Global cancer in women, burden and trends. *Cancer Epidemiol. Biomarkers Prev.* **2017**, *26*, 444–457. [[CrossRef](#)] [[PubMed](#)]
5. Ellsworth, R.E.; Blackburn, H.L.; Shriver, C.D.; Soon-Shiong, P.; Ellsworth, D.L. Molecular heterogeneity in breast cancer, State of the science and implications for patient care. *Semin. Cell. Dev. Biol.* **2017**, *64*, 65–72. [[CrossRef](#)] [[PubMed](#)]
6. Prasetyanti, P.R.; Medema, J.P. Intra-tumor heterogeneity from a cancer stem cell perspective. *Mol. Cancer* **2017**, *16*, 41. [[CrossRef](#)]
7. Aponte, P.M.; Caicedo, A. Stemness in cancer, Stem cells, cancer stem cells, and their microenvironment. *Stem Cells Int.* **2017**, *2017*, 5619472. [[CrossRef](#)]
8. Pazdur, R.; Kudelka, A.P.; Kavanagh, J.J.; Cohen, P.R.; Raber, M.N. The taxoids, paclitaxel (Taxol) and docetaxel (Taxotere). *Cancer Treat Rev.* **1993**, *19*, 351–386. [[CrossRef](#)]
9. Perez, E.A. Paclitaxel in Breast Cancer. *Oncologist* **1998**, *3*, 373–389.
10. Gudena, V.; Montero, A.J.; Glück, S. Gemcitabine and taxanes in metastatic breast cancer, a systematic review. *Ther. Clin. Risk Manag.* **2008**, *4*, 1157–1164.

11. Klimaszewska-Wisniewska, A.; Halas-Wisniewska, M.; Tadrowski, T.; Gagat, M.; Grzanka, D.; Grzanka, A. Paclitaxel and the dietary flavonoid fisetin, a synergistic combination that induces mitotic catastrophe and autophagic cell death in A549 non-small cell lung cancer cells. *Cancer Cell. Int.* **2016**, *16*, 1. [[CrossRef](#)] [[PubMed](#)]
12. Rivera, E.; Gomez, H. Chemotherapy resistance in metastatic breast cancer, the evolving role of ixabepilone. *Breast Cancer Res.* **2010**, *12* (Suppl. 2). [[CrossRef](#)] [[PubMed](#)]
13. Toppmeyer, D.; Seidman, A.D.; Pollak, M.; Russell, C.; Tkaczuk, K.; Verma, S.; Overmoyer, B.; Garg, V.; Ette, E.; Harding, M.W.; et al. Safety and efficacy of the multidrug resistance inhibitor Incel (biricodar, VX-710) in combination with paclitaxel for advanced breast cancer refractory to paclitaxel. *Clin. Cancer Res.* **2002**, *8*, 670–678. [[PubMed](#)]
14. Gill, C.; Walsh, S.E.; Morrissey, C.; Fitzpatrick, J.M.; Watson, R.W. Resveratrol sensitizes androgen independent prostate cancer cells to death-receptor mediated apoptosis through multiple mechanisms. *Prostate* **2007**, *67*, 1641–1653. [[CrossRef](#)]
15. Tolba, M.F.; Esmat, A.; Al-Abd, A.M.; Azab, S.S.; Khalifa, A.E.; Mosli, H.A.; Abdel-Rahman, S.Z.; Abdel-Naim, A.B. Caffeic acid phenethyl ester synergistically enhances docetaxel and paclitaxel cytotoxicity in prostate cancer cells. *IUBMB Life* **2013**, *65*. [[CrossRef](#)]
16. El-Araby, M.E.; Omar, A.M.; Khayat, M.T.; Assiri, H.A.; Al-Abd, A.M. Molecular mimics of classic p-glycoprotein inhibitors as multidrug resistance suppressors and their synergistic effect on paclitaxel. *PLoS ONE* **2017**, *12*. [[CrossRef](#)]
17. Dastjerdi, M.N.; Mehdiabady, E.M.; Iranpour, F.G.; Bahramian, H. Effect of Thymoquinone on P53 Gene Expression and Consequence Apoptosis in Breast Cancer Cell Line. *Int. J. Prev. Med.* **2016**, *7*, 66. [[CrossRef](#)]
18. Ahmad, A.; Husain, A.; Mujeeb, M.; Alam Khan, S.; Najmi, A.K.; Siddique, N.A.; Damanhoury, Z.A.; Anwar, F.; Kishore, K. A review on therapeutic potential of Nigella sativa, A miracle herb. *Asian Pac. J. Trop Biomed.* **2013**, *3*, 337–352. [[CrossRef](#)]
19. Kassab, R.B.; El-Hennamy, R.E. The role of thymoquinone as a potent antioxidant in ameliorating the neurotoxic effect of sodium arsenate in female rat. *Egypt J. Basic Appl. Sci.* **2017**, *4*, 160–167. [[CrossRef](#)]
20. Randhawa, M.A.; Alenazy, A.K.; Alrowaili, M.G.; Basha, J. An active principle of Nigella sativa L., thymoquinone, showing significant antimicrobial activity against anaerobic bacteria. *J. Intercult. Ethnopharmacol.* **2017**, *6*, 97–101. [[CrossRef](#)]
21. Abd El Aziz, A.E.; El Sayed, N.S.; Mahran, L.G. Anti-asthmatic and Anti-allergic effects of Thymoquinone on Airway-Induced Hypersensitivity in Experimental Animals. *J. Appl. Pharm. Sci.* **2011**, *1*, 109–117.
22. Mostofa, A.G.M.; Hossain, M.K.; Basak, D.; Bin Sayeed, M.S. Thymoquinone as a Potential Adjuvant Therapy for Cancer Treatment, Evidence from Preclinical Studies. *Front. Pharmacol.* **2017**, *8*, 295. [[CrossRef](#)] [[PubMed](#)]
23. Mokhtari, R.B.; Homayouni, T.S.; Baluch, N.; Morgatskaya, E.; Kumar, S.; Das, B.; Yeager, H. Combination therapy in combating cancer. *Oncotarget* **2017**, *8*, 38022–38043. [[CrossRef](#)] [[PubMed](#)]
24. Ghoncheh, M.; Pournamdar, Z.; Salehiniya, H. Incidence and Mortality and Epidemiology of Breast Cancer in the World. *Asian Pac. J. Cancer Prev.* **2016**, *17*, 43–46. [[CrossRef](#)]
25. Miura, D.; Yoneyama, K.; Furuhashi, Y.; Shimizu, K. Paclitaxel Enhances Antibody-dependent Cell-mediated Cytotoxicity of Trastuzumab by Rapid Recruitment of Natural Killer Cells in HER2-positive Breast Cancer. *J. Nippon. Med. Sch.* **2014**, *81*, 211–220. [[CrossRef](#)]
26. Dorman, S.N.; Baranova, K.; Knoll, J.H.; Urquhart, B.L.; Mariani, G.; Carcangiu, M.L.; Rogan, P.K. Genomic signatures for paclitaxel and gemcitabine resistance in breast cancer derived by machine learning. *Mol. Oncol.* **2016**, *10*, 85–100. [[CrossRef](#)]
27. Barbuti, A.M.; Chen, Z.-S. Paclitaxel Through the Ages of Anticancer Therapy, Exploring Its Role in Chemoresistance and Radiation Therapy. *Cancers (Basel)* **2015**, *7*, 2360–2371. [[CrossRef](#)]
28. Khader, M.; Eckl, P.M. Thymoquinone, an emerging natural drug with a wide range of medical applications. *Iran J. Basic Med. Sci.* **2014**, *17*, 950–957.
29. Jafri, S.H.; Glass, J.; Shi, R.; Zhang, S.; Prince, M.; Kleiner-Hancock, H. Thymoquinone and cisplatin as a therapeutic combination in lung cancer, In vitro and in vivo. *J. Exp. Clin. Cancer Res.* **2010**, *29*, 87. [[CrossRef](#)]
30. Zhang, L.; Bai, Y.; Yang, Y. Thymoquinone chemosensitizes colon cancer cells through inhibition of NF- κ B. *Oncol. Lett.* **2016**, *12*, 2840–2845. [[CrossRef](#)]

31. Alaufi, O.M.; Noorwali, A.; Zahran, F.; Al-Abd, A.M.; Al-Attas, S. Cytotoxicity of thymoquinone alone or in combination with cisplatin (CDDP) against oral squamous cell carcinoma in vitro. *Sci. Rep.* **2017**, *7*. [[CrossRef](#)] [[PubMed](#)]
32. Bashmail, H.A.; AlAmoudi, A.A.; Noorwali, A.; Hegazy, G.A.; Ajabnoor, G.; Choudhry, H.; Al-Abd, A.M. Thymoquinone synergizes gemcitabine anti-breast cancer activity via modulating its apoptotic and autophagic activities. *Sci. Rep.* **2018**, *8*, 11674. [[CrossRef](#)] [[PubMed](#)]
33. Han, W.B.; Lu, Y.H.; Zhang, A.H.; Zhang, G.F.; Mei, Y.N.; Jiang, N.; Lei, X.; Song, Y.C.; Ng, S.W.; Tan, R.X. Curvulamine, a new antibacterial alkaloid incorporating two undescribed units from a *Curvularia* species. *Org. Lett.* **2014**, *16*, 5366–5369. [[CrossRef](#)] [[PubMed](#)]
34. Takeishi, S.; Nakayama, K.I. To wake up cancer stem cells, or to let them sleep, that is the question. *Cancer Sci.* **2016**, *107*, 875–881. [[CrossRef](#)] [[PubMed](#)]
35. Alobaedi, O.H.; Talib, W.H.; Basheti, I.A. Antitumor effect of thymoquinone combined with resveratrol on mice transplanted with breast cancer. *Asian Pac. J. Trop. Med.* **2017**, *10*, 400–408. [[CrossRef](#)] [[PubMed](#)]
36. Ganji-Harsini, S.; Khazaei, M.; Rashidi, Z.; Ghanbari, A. Thymoquinone Could Increase The Efficacy of Tamoxifen Induced Apoptosis in Human Breast Cancer Cells, An In Vitro Study. *Cell J.* **2016**, *18*, 245–254. [[CrossRef](#)]
37. Şakalar, Ç.; İzgi, K.; İskender, B.; Sezen, S.; Aksu, H.; Çakır, M.; Kurt, B.; Turan, A.; Canatan, H. The combination of thymoquinone and paclitaxel shows anti-tumor activity through the interplay with apoptosis network in triple-negative breast cancer. *Tumor Biol.* **2016**, *37*, 4467–4477. [[CrossRef](#)]
38. Jänicke, R.U. MCF-7 breast carcinoma cells do not express caspase-3. *Breast Cancer Res. Treat.* **2009**, *117*, 219–221. [[CrossRef](#)]
39. Zhao, J. Cancer stem cells and chemoresistance, The smartest survives the raid. *Pharmacol. Ther.* **2016**, *160*, 145–158. [[CrossRef](#)]
40. Horimoto, Y.; Arakawa, A.; Sasahara, N.; Tanabe, M.; Sai, S.; Himuro, T.; Saito, M. Combination of Cancer Stem Cell Markers CD44 and CD24 Is Superior to ALDH1 as a Prognostic Indicator in Breast Cancer Patients with Distant Metastases. *PLoS ONE* **2016**, *11*, e0165253. [[CrossRef](#)]
41. Alfarouk, K.O.; Stock, C.-M.; Taylor, S.; Walsh, M.; Muddathir, A.K.; Verduzco, D.; Bashir, A.H.H.; Mohammed, O.Y.; O ElHassan, G.; Harguindey, S.; et al. Resistance to cancer chemotherapy, failure in drug response from ADME to P-gp. *Cancer Cell Int.* **2015**, *15*, 71. [[CrossRef](#)] [[PubMed](#)]
42. Spaeth, E.L.; Labaff, A.M.; Toole, B.P.; Klopp, A.; Andreeff, M.; Marini, F.C. Mesenchymal CD44 expression contributes to the acquisition of an activated fibroblast phenotype via TWIST activation in the tumor microenvironment. *Cancer Res.* **2013**, *73*, 5347–5359. [[CrossRef](#)] [[PubMed](#)]
43. Khan, A.; Tania, M.; Wei, C.; Mei, Z.; Fu, S.; Cheng, J.; Xu, J.; Fu, J. Thymoquinone inhibits cancer metastasis by downregulating TWIST1 expression to reduce epithelial to mesenchymal transition. *Oncotarget* **2015**, *6*, 19580. [[CrossRef](#)] [[PubMed](#)]
44. Brabletz, T.; Jung, A.; Spaderna, S.; Hlubek, F.; Kirchner, T. Migrating cancer stem cells—An integrated concept of malignant tumour progression. *Nat. Rev. Cancer* **2005**, *5*, 744. [[CrossRef](#)] [[PubMed](#)]
45. Tamura, D.; Arao, T.; Nagai, T.; Kaneda, H.; Aomatsu, K.; Fujita, Y.; Matsumoto, K.; De Velasco, M.A.; Kato, H.; Hayashi, H.; et al. Slug increases sensitivity to tubulin-binding agents via the downregulation of β III and β IVa-tubulin in lung cancer cells. *Cancer Med.* **2013**, *2*, 144–154. [[CrossRef](#)] [[PubMed](#)]
46. Skehan, P.; Scudiero, M.; Vistica, D.; Bokesch, H.; Kenney, S.; Storeng, R.; Monks, A.; McMahon, J.; Warren, J.T.; Boyd, M.R. New colorimetric cytotoxicity assay for anticancer-drug screening. *J. Natl. Cancer Inst.* **1990**, *82*, 1107–1112. [[CrossRef](#)] [[PubMed](#)]
47. Chou, T.C.; Talalay, P. Generalized equations for the analysis of inhibitions of Michaelis-Menten and higher-order kinetic systems with two or more mutually exclusive and nonexclusive inhibitors. *Eur. J. Biochem.* **1981**, *115*, 207–216. [[CrossRef](#)]

Sample Availability: Samples of the used compounds are available from the authors.



© 2020 by the authors. Licensee MDPI, Basel, Switzerland. This article is an open access article distributed under the terms and conditions of the Creative Commons Attribution (CC BY) license (<http://creativecommons.org/licenses/by/4.0/>).